M&C 2017 - International Conference on Mathematics & Computational Methods Applied to Nuclear Science & Engineering, Jeju, Korea, April 16-20, 2017, on USB (2017)

Validation of Selected IRDFF Cross Sections in Well-Defined Rector Spectrum

Michal Košťál, Evžen Losa, Vojtěch Rypar, Davit Harutyunyan, Martin Schulc

Research Centre Rez Ltd, 250 68 Husinec-Rez 130, Czech Republic, Michal.Kostal@cvrez.cz

Abstract - *The paper describes validation of the (n,2n) reaction rates of selected IRDFF materials, namely ^{23}Na and ^{75}As in a well-defined reactor spectrum of special core assembled in the LR-0 reactor. The reaction rates are derived from activity of ^{22}Na and ^{74}As activation product which is determined using gamma spectroscopy of irradiated samples. The resulted values are compared with calculations which were carried out with the MCNP6 code using ENDF/B-VII.0, ENDF/V-VII.1, JEFF-3.1, JEFF-3.2, JENDL-3.3, JENDL-4, ROSFOND-2010 and CENDL-3.1 nuclear data libraries. The agreement is relatively good for $^{75}As(n,2n)$, notably worse for $^{23}Na(n,2n)$. Significant improvement of results can be seen when CIELO evaluation of prompt fission neutron spectra of both ^{235}U and ^{238}U are used. The experimental uncertainties are below 5 %, thus meeting the EXFOR requirements.*

I. INTRODUCTION

Testing, improvement, and validation of selected dosimetric cross sections from IRDFF library (International Reactor Dosimetry and Fusion File) is an on-going Coordinated Research Project (CRP) organized by the International Atomic Energy Agency (IAEA). The need for validation and improvement of the current energy integrated as well as differential data rises from the fact that the results in EXFOR are either old, have high uncertainties, or are missing for specific energies. Reactions $^{23}Na(n,2n)^{22}Na$ and $^{75}As(n,2n)^{74}As$ belong to those demanded to be verified, because they can be used as neutron flux monitors.

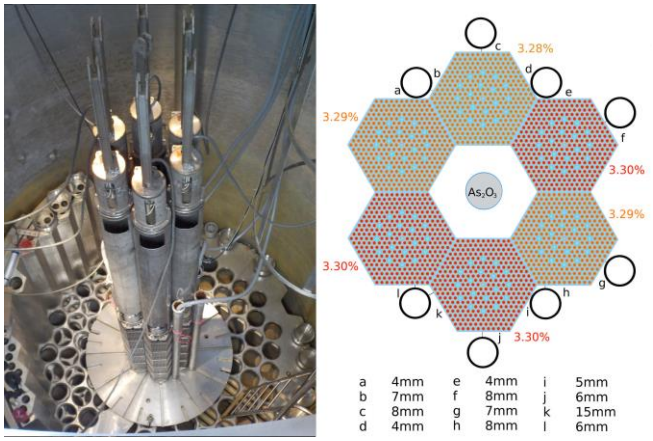

Fig. 1: Overhead view inside the LR-0 reactor with dry special core (left) and radial plot of the core with specified enrichment for each assembly (right).

II. DESCRIPTION OF THE ACTUAL WORK

This article presents neutron cross sections validation measurements of (n,2n) reactions averaged in reactor spectrum. Spectrum Averaged Cross-Sections (SACS hereafter) are derived from experimentally determined reaction rates (RR hereafter) after sample irradiation in the zero power reactor LR-0 at the Research Centre Řež, in the Czech Republic. Determination of RR is based on the gamma spectrum Net Peak Areas (NPA) of photons accompanying the decay of observed product, measured using a semiconductor High Purity Germanium (HPGe) detector. Both products, ^{22}Na and ^{74}As, could theoretically origin from (γ,n) reactions as well, but it is shown that this channel has γ threshold higher than the most energetic part of the photon spectrum in used fission reactor core.

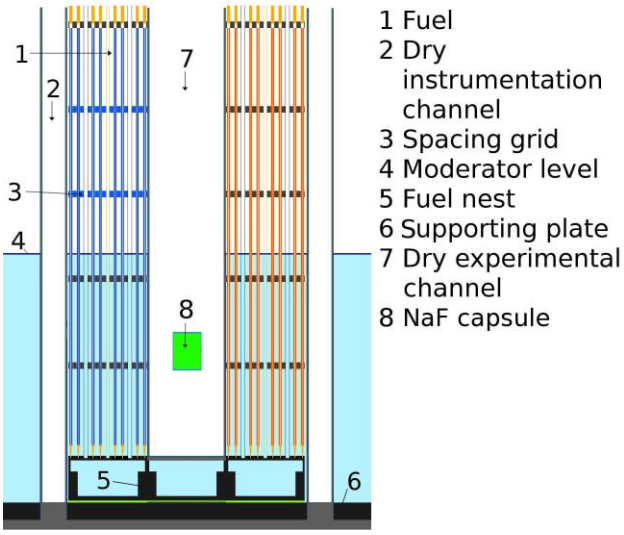

Fig. 2: Axial plot of core in Na measurement

1. Reactor Arrangement

Current LR-0 reactor core with 3.3 % LEU fuel (see Fig. 1) can be considered as a well-defined neutron source, because it was exactly described in terms of criticality [1], fission density in fuel [2] and neutron spectrum [3] (see Fig.3). Its advantage is that the neutron field in irradiation channel (see Fig. 1 right) can be considered as homogenous and therefore large and thick targets can be used for experiments. Fig. 2 shows the axial section of configuration used for cross section validations.

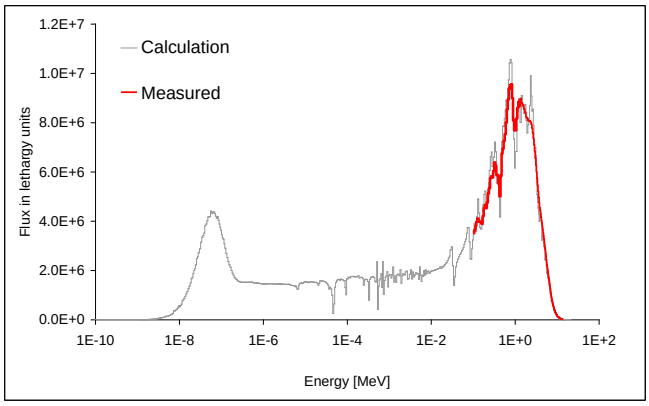

Fig. 3: Comparison of calculated and measured neutron flux in the same core arrangement (detector is placed instead of sample) in lethargy units

Irradiated materials had form compatible with light water reactor emergency scenarios (Na in form of the NaF salt, As in form of densified As_2O_3) and were placed into large aluminum capsules. The net weight of irradiated NaF was 644 g and 657 g in case of As_2O_3.

2. Gamma Spectroscopy of Irradiated Target

Gamma spectroscopy was used for the determination of the reaction product, ^{22}Na and ^{74}As, amount in the irradiated sample. In case of NaF, the sample was placed into Marinelli beaker (see Fig. 5), in case of As_2O_3 it was placed in hermetic capsule due to high toxicity of arsenic. Configuration of the arsenic sample gamma spectrometry is shown in Fig. 6. The SACS is determined from reaction rate of activation product (see Eq. 1.) The reaction rate is calculated from activity by division by efficiency, branch ratio and is corrected to decay during irradiation, following decay time, and measurement time as well (see Eq. 2).

The efficiency of the apparatus was determined calculationally. The computational model was compiled using detector parameters indirectly measured in HPGe radiogram [7], (see Fig. 7). This characterization of HPGe is very important, because variations between responses of calculation models using experimental and producer data can be as high as 30 % [8]. The calculation model was finally verified by point etalon sources containing ^{241}Am, ^{57}Co, ^{60}Co, ^{137}Cs, ^{113}Sn, ^{85}Sr and ^{88}Y and volume source with ^{137}Cs, ^{60}Co, ^{241}Am. The geometry was selected to be similar to geometry used in measurement (see Fig. 4). Obtained bias, being uncertainty in HPGe modeling and simplifications is not higher than 1.9 % in case of ^{22}Na measurement in configuration with Marinelli beaker (see Fig. 4). The bias can be slightly higher, when other geometry is used as it in case of ^{74}As measurement (see Fig. 6).

The observed products origin not only from the (n,2n) reaction, but also from (γ,n) reaction. After irradiation, it is not possible to distinguish between both. The calculation using ENDF/B-VII.0 data shows that the contribution from (γ,n) is negligible, because its threshold is above the most energetic part of the photon spectrum [4,5] in nuclear reactor.

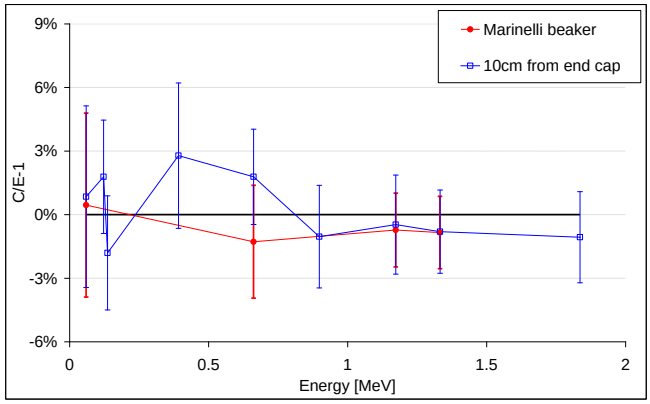

Fig. 4: Bias between calculation and experiment for volume source measurement arrangement (^{74}As and ^{22}Na)

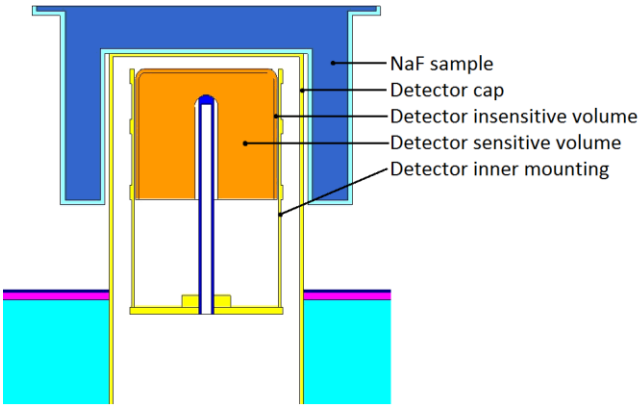

Fig. 5: NaF measuring arrangement in configuration with Marinelli beaker

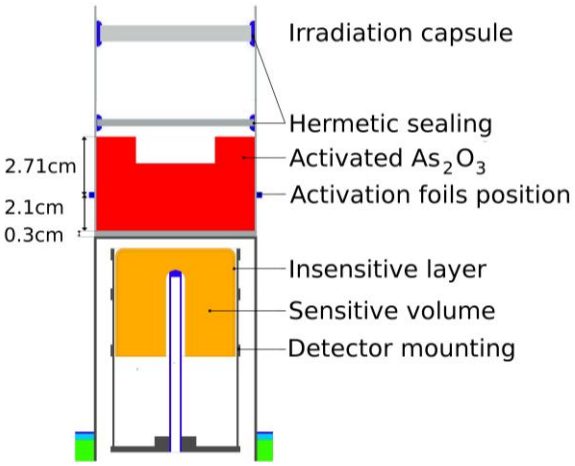

Fig. 6: Schematic of irradiated As_2O_3 measurement method.

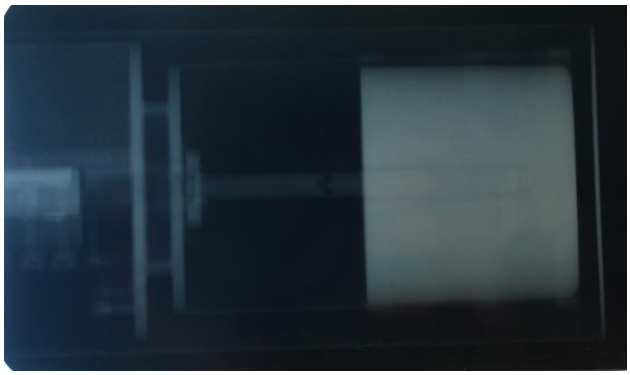

Fig. 7: Radiogram of HPGe used for model compilation

3. Flux normalization

The SACS can be derived from RR when normalized to neutron flux. The flux is determined by means of calculation using experimentally determined scaling factor (see Eq. 3). The scaling factor, which is in fact neutron emission rate, was determined by set of activation foils (Au, Ni). Their effect on neutronics in irradiated sample is negligible because of small dimensions, diameter: 3.6 mm, and thickness: 0.1 mm. Foils were attached to the capsule with irradiated material. In case of As_2O_3 capsule at the height 2.4 cm above the lower end along the axial axis, in the Na case 5.6 cm.

To decrease the uncertainty, six Au foils and three Ni foils were used. Foils were placed in radially symmetric positions (Au in 60 deg symmetry, Ni in 120 deg symmetry). The irradiated activation foils were measured by the gamma-spectrometric device with the HPGe detector, same as was used in irradiated Na and As. More details can be found above.

The foil activity measurement started immediately after the end of irradiation. In the irradiated Au foil, the spectrum was evaluated for the 411.8 keV peak of ^{198}Au originating from the ^{197}Au(n,γ) reaction. In the irradiated Ni foil, the 810.8 keV peak of ^{58}Co originating from the ^{58}Ni(n,p) reaction was examined. The parameters of the activation materials used are listed in Table I.

Table I. C/E-1 summary of monitor materials

Activation material	^{198}Au	^{58}Co
Reaction	^{197}Au(n,γ)	^{58}Ni(n,p)
Gamma line [keV]	411.8	810.8
Branching ratio	0.9562	0.9945
$T_{1/2}$	2.6947 d	70.86 d
Efficiency	2.59E-2	4.63E-2
RR for Na irradiation	4.93E-15	2.86E-18
RR for As irradiation	4.24E-15	2.38E-18

The efficiency calibration curve of the HPGe detector was calculated using the MCNP6 code using experimentally obtained parameters of detector which was verified in the same measurement geometry. The Calculated/Experimental agreement C/E for the point etalon sources in the end cap experimental geometry used in activation foil measurement is presented in Fig. 8. The RR was determined from NPA using following equation:

$$SACS = \bar{\sigma} = \frac{q(\bar{\mathrm{P}})}{\int_{\mathrm{E}>10\,\mathrm{MeV}} \varphi(\mathrm{E}) \times d\mathrm{E}} \tag{1}$$

$$q(\bar{\mathrm{P}}) = \frac{C(\mathrm{T}_m)}{\frac{A(\bar{\mathrm{P}})}{A_{\mathrm{Sat}}(\bar{\mathrm{P}})}} \times \frac{\lambda}{\varepsilon \times \eta \times N} \times \frac{1}{\left(1 - e^{-\lambda.\mathrm{T}_m}\right)} \times \frac{1}{e^{-\lambda.\Delta\mathrm{T}}} \tag{2}$$

The scaling factor is determined from comparison of experimental and calculated reaction rates of monitoring foils (see Eq. 3). Its physical meaning is the neutron emission rate of the reactor core. It is worth noting that the average scaling factors in both independent experiments determined from Au and Ni vary from one another approximately by 2.5 % in case of Na or about 1 % in case of As. Assuming that all presented sources of uncertainty are non-correlated, the total uncertainty is determined as square root of the sum of the squares of all combined uncertainties, and in these cases it makes 2 - 3 %.

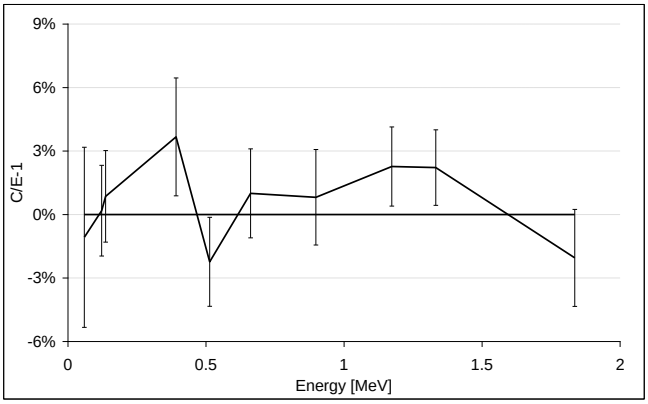

Fig. 8: Bias between calculation and experiment for foil measurement arrangement

The scaling factor used for the absolute neutron flux evaluation can be described by the following equation:

$$K = \frac{K_{\mathrm{Au}} + K_{\mathrm{Ni}}}{2} \qquad (3)$$

Where:

K_{Au} ; is the scaling factor determined from the Au RR and $K_{\mathrm{Au}} = \sum_{i=1}^{N} \frac{q_{\mathrm{Au}}^{i}(1\,\mathrm{nps})_{\mathrm{Calculated}}}{q_{\mathrm{Au}}^{i}(\overline{\mathrm{P}})_{\mathrm{Measured}}}$;

K_{Ni} ; is the scaling factor determined from Ni RR and $K_{\mathrm{Ni}} = \sum_{i=1}^{N} \frac{q_{\mathrm{Ni}}^{i}(1\,\mathrm{nps})_{\mathrm{Calculated}}}{q_{\mathrm{Ni}}^{i}(\overline{\mathrm{P}})_{\mathrm{Measured}}}$;

K ; is the scaling factor used in the following evaluations;

4. Calculations

Additionally to the experiment, calculations of neutron transport from core to irradiated sample and photon transport covering transport of photons to detector were realized using MCNP6 Monte Carlo code. The computing model of the reactor core was compiled based on precise description of core, which is included in IRPhEP benchmark database. Irradiated targets were modelled using selected nuclear data libraries: ENDF/B-VII.0, ENDF/B-VII.1, JEFF-3.1, JEFF-3.2, JENDL-4, JENDL-3.3, RUSFOND-2010 and CENDL-3.1. Reactor core definition was fixed in the ENDF/B-VII.0 library and in CIELO library. CIELO was chosen due to the lower reported discrepancies in prompt fission neutron spectrum of ^{235}U [6]. Differences in prompt fission neutron spectrum (PFNS) of both CIELO and ENDF/B-VII.0 can be seen on plot in Fig. 11.

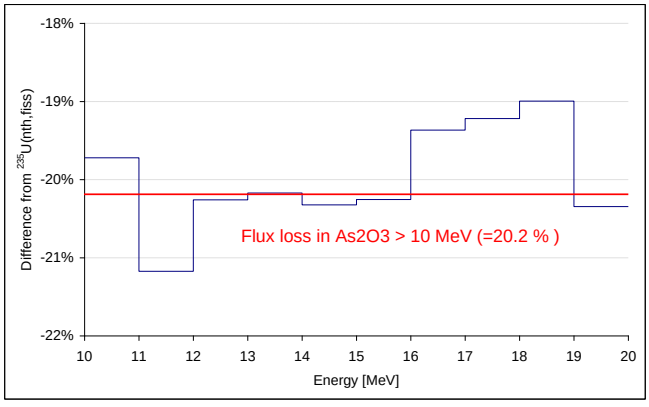

Fig. 9: Spectral shift and flux loss for As_2O_3 target

Neutron transport, namely activation of foils and studied samples, was simulated in the criticality model. Satisfactory agreement of the calculated k_{eff} for a model using the experimentally determined critical configuration was obtained with resulting effective multiplication factors of 1.002 for Na and 1.003 for As. This indicates that the fission source uncertainty plays only a minor role in the obtained RR results. RR was normalized to the source neutrons by dividing the RR by the calculated k_{eff}. Normalization to the real neutron flux level is performed via multiplication by the scaling factor calculated from the RR in activation foils.

The experimentally derived SACS is also corrected to the self-shielding effect, which was identified as a ratio between the SACS in the full geometry used for irradiation and the SACS which would be virtually obtained in the geometrically identical but empty geometry (without irradiated sample in the model). The resulting ratio was determined by Monte Carlo simulation as the ratio of SACS in real sample. For increasing of the calculational accuracy the isotropic field of prompt fission of ^{235}U(n.th,fiss) was used. Resulted self-shielding correction factor is in both cases close to 1, namely 0.999 for Na and 1.003 for As, which indicates that the change in SACS due to the spectral shift is negligible. The detailed calculational comparison of spectral shift and flux loss is presented in Fig. 9 for As_2O_3 target and in Fig. 10 for NaF target.

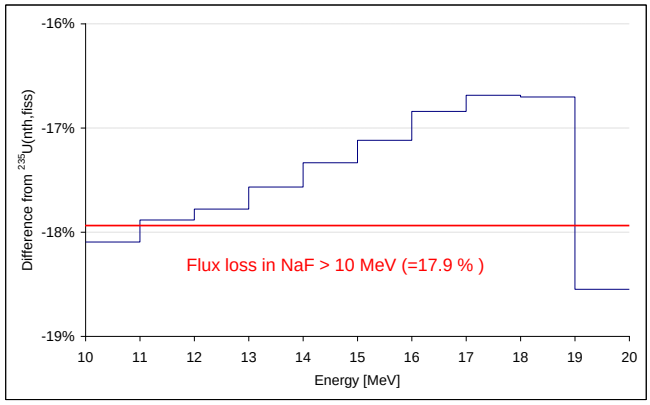

Fig. 10: Spectral shift and flux loss for NaF target

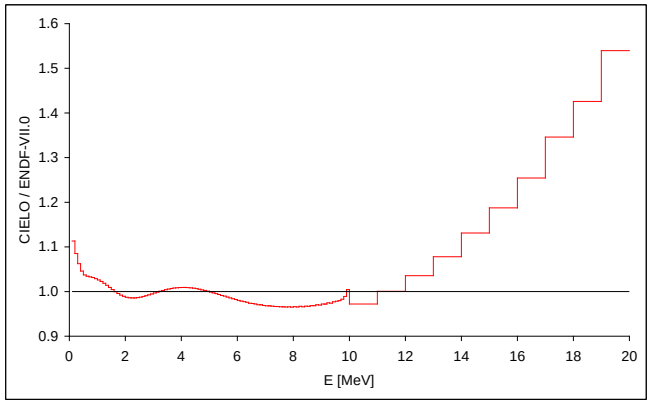

Fig. 11: Comparison between ENDF/B-VII and CIELO libraries for prompt fission spectrum of ^{235}U

III. RESULTS

Both, experimental and calculated RR are listed below in Table II. The SACS of ^{23}Na(n,2n) is notably smaller than ^{75}As(n,2n) because of its notably higher threshold and smaller cross section. Thus it can be assumed that ^{23}Na(n,2n) is more sensitive to higher neutron energies than ^{75}As(n,2n). The comparison between calculated and measured ^{75}As(n,2n) and ^{23}Na(n,2n) RR in prompt fission neutron spectrum defined by ENDF/B-VII.0 library is listed in Table III. The same comparison, but using the CIELO PFNS definition is shown in Table IV. It can be concluded that arsenic results are in remarkably better agreement than sodium ones, independently on used fission spectrum definition. It is worth noting, when using PFNS described by CIELO, that the agreement is getting better. It seems that due to higher energy at which the 50 % of reaction rate is produced ($E_{50\%}$) at ^{23}Na(n,2n), higher variations between calculated RR with PFNS of CIELO or ENDF-B/VII.0 can be seen for ^{23}Na(n,2n), than for ^{75}As(n,2n) reaction. It is given by large discrepancies occurring between ENDF/B-VII and CIELO PFNS evaluations in higher energies (see Fig. 11). The cross sections in different libraries are plotted in Fig. 12 and Fig. 13 respectively.

Table II. Summary of results

	^{23}Na(n,2n)	^{75}As(n,2n)	
Measured activity	0.553	785	[Bq]
Experimental RR	2.05E-34	6.40E-21	[1/s]
Neutron emission rate	4.54E+11	3.99E+11	[1/s]
Correction to spectral shift	0.991	1.003	[-]
SACS in reactor spectrum > 10 MeV	2.86	237	[mb]
SACS in reactor spectrum > 10 MeV	0.955	80.2	[mb]
SACS in ^{235}U PFNS	0.00396	0.332	[mb]
E 50%	15.23	12.67	[MeV]
Uncertainty	4.1%	4.1%	[-]

Table III. C/E-1 of RR calculated with ENDF/B-VII.0 PFNS

	^{23}Na(n,2n)	^{75}As(n,2n)
ENDF/B-VII.0	33.1%	1.16%
ENDF/B VII.1	33.1%	-1.31%
JEFF-3.1	-14.8%	0.00%
JEFF-3.2	-0.3%	-1.95%
JENDL-3.3	-14.9%	-7.28%
JENDL-4	-14.9%	1.07%
RUSFOND-2010	-7.0%	-7.28%
CENDL-3.1	-2.7%	1.43%
IRDFF	-12.5%	-4.0%

Table IV. C/E-1 of RR calculated with CIELO PFNS

	^{23}Na(n,2n)	^{75}As(n,2n)
ENDF/B-VII.0	63.0%	3.74%
ENDF/B-VII.1	63.0%	1.55%
JEFF-3.1	1.1%	-
JEFF-3.2	20.8%	0.81%
JENDL-3.3	2.1%	-4.59%
JENDL-4	2.1%	3.78%
RUSFOND-2010	11.4%	-4.59%
CENDL-3.1	16.3%	4.28%
IRDFF	6.7%	-1.2%

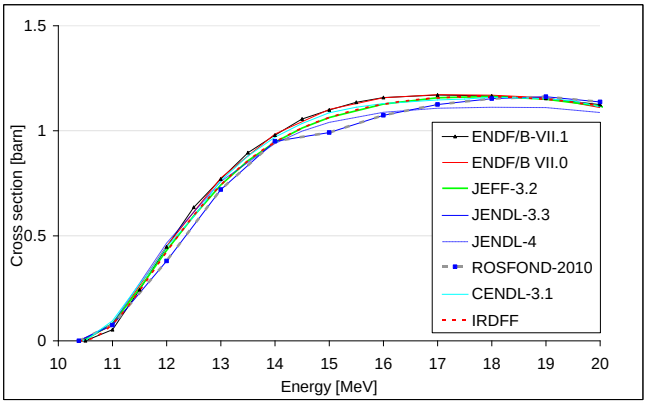

Fig. 12: ^{75}As(n,2n) cross section in various libraries

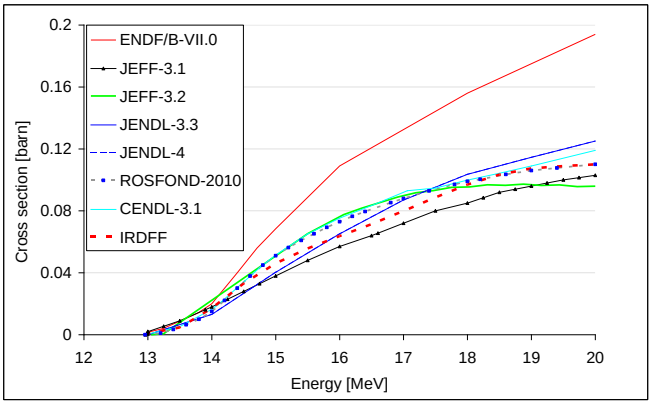

Fig. 13: ^{23}Na(n,2n) cross section in various libraries

IV. CONCLUSIONS

The measurement of both ^{75}As(n,2n)^{74}As and ^{23}Na(n,2n)^{22}Na reaction rates and evaluation of SACS has demonstrated the reliability of the equipment in the LR-0 laboratory for neutron cross sections validation.

In this work, the cross section of the ^{75}As(n,2n) and ^{23}Na(n,2n) reactions were derived from measured data. Resulting values are 332 μb for ^{75}As and 3.96 μb, for ^{23}Na. The experimental results for ^{75}As(n,2n) are in quite good agreement with the calculations in wide range of nuclear data libraries, and in satisfactory agreement with previous

measurement in EXFOR 0.311 ±0.023 mb [9]. In the case of ^{23}Na(n,2n), the agreement is much worse, as the discrepancies are higher than in the other case. Usage of CIELO fission spectrum description improves the agreement in IRDFF library, recommended for calculations of activation.

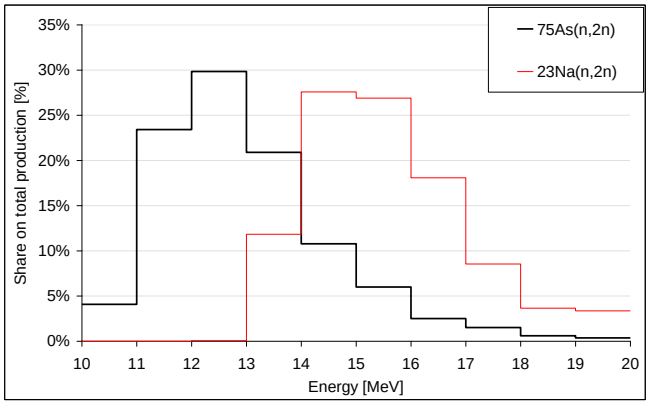

Fig. 14: Energy distribution of studied nuclear reactions.

The variations between PFNS in ENDF/B-VII.0 and CIELO are bigger in higher energy regions, thus more notable change in SACS occurs in case of ^{23}Na(n,2n), as it presents a higher $E_{50\%}$ than ^{75}As(n,2n).

NOMENCLATURE

$q(\overline{P})$	= reaction rate of activation during defined power density
T_m	= time of measurement by HPGe;
ΔT	= time between the end of irradiation and the start of HPGe measurement;
$C(T_m)$	the measured number of counts;
ε	= gamma branching ratio;
η	= detector efficiency (the result of MCNP6 calculation);
N	= number of target isotope nuclei;
$q(\overline{P})$	= reaction rate of activation during power density
$\frac{A(\overline{P})}{A_{Sat}(\overline{P})}$	$= \sum_i P_{rel}^i \times \left(1-e^{-\lambda.T_{Irr}^i}\right) \times e^{-\lambda.T_{end}^i}$
P_{rel}^i	= relative power in i-th interval of the irradiation period $P_{rel}^i = P^i / \overline{P}$
T_{ir}^i	= irradiation time in i-th interval of the irradiation period
T_{end}^i	= time from the end of the i-th irradiation interval to the reference time (end of irradiation period)
λ	= decay constant of the radioisotope considered
$\overline{P}$	= mean power with defined neutron emission rate is 3.88×10^{11} neutrons/s

ACKNOWLEDGMENTS

The presented work was financially supported by the Ministry of Education, Youth and Sport Czech Republic Project LQ1603 (Research for SUSEN). This work has been realized within the SUSEN Project (established in the framework of the European Regional Development Fund (ERDF) in project CZ.1.05/2.1.00/03.0108). The authors would like to thank to the staff of the LR-0 reactor, headed by J. Milcak, for their effective help during the experiments and for the precise monitoring of the reactor power.

REFERENCES

1. M. KOŠŤÁL, V. RYPAR, J. MILČÁK et al., Study of graphite reactivity worth on well-defined cores assembled on LR-0 reactor, *Ann. of Nucl. En.*, **87**, (2016), pp 601-611
2. M. KOŠŤÁL, M. ŠVADLENKOVÁ, P. BAROŇ et al, Determining the axial power profile of partly flooded fuel in a compact core assembled in reactor LR-0, *Ann. of Nucl. En.*, **90**, (2016), pp 450-458
3. M. KOŠŤÁL, M. VEŠKRNA, F. CVACHOVEC et al, Comparison of fast neutron spectra in graphite and FLINA salt inserted in well-defined core assembled in LR-0 reactor, *Ann. of Nucl. En.*, **83**, (2015), pp. 216-225
4. M. KOŠŤÁL, M. ŠVADLENKOVÁ, P. BAROŇ et al, Measurement of 23Na(n,2n) cross section in well-defined reactor spectra, *Appl. Rad. and Isot.*, **111**, (2016), pp 1-7
5. M. KOŠŤÁL, V. RYPAR, M. SCHULC et al, Measurement of 75As(n,2n) cross section in well-defined spectrum of LR-0 special core, *Ann. of Nucl. En.*, **100**, (2017), pp. 42-49
6. R. Capote, A. Trkov, M. Sin, M.W. Herman, V.G. Pronyaev; Mini-CSWEG, 11-12 April 2016, LANL, Los Alamos, USA, (https://www-nds.iaea.org/CIELO/Capote-miniCSWEG2016-u235.pdf)
7. Pavel Dryak, Petr Kovar, Experimental and MC determination of HPGe detector efficiency in the 40–2754 keV energy range for measuring point source geometry with the source-to-detector distance of 25 cm, *Appl. Rad. and Isot.*, 64, **2006**, pp 1346-1349
8. Jonas Boson, Göran Ågren, Lennart Johansson A detailed investigation of HPGe detector response for improved Monte Carlo efficiency calculations, Nuclear Instruments and Methods in Physics Research Section A: Accelerators, Spectrometers, Detectors and Associated Equipment, 587, **2008**, pp 304-314
9. F. Nasyrov, B.D. Sciborskij, Atomnaja Energija, v.25, no.5, p.437, November 1968